

RESEARCH LETTER

Open Access



# The Makkah–Madinah Transform Zone: a relic rift-to-rift continental transform formed during early Arabia–Nubia plate separation

Thamer Aldaajani<sup>1,2\*</sup>  and Kevin P. Furlong<sup>1</sup>

## Abstract

The continental-rifting of Arabia from Nubia, and the initial evolution of the Red Sea spreading center includes many of the continental-rifting to ocean-spreading processes, in particular transform formation, and the eventual development of a mid-ocean ridge. The recent occurrence of this rifting and the multi-stage evolution of the plate boundary has preserved key components of the early-stage plate boundary development. We find that the Makkah–Madinah Transform Zone (MMTZ) represents a rift-to-rift continental transform fault that served as a primary component of the initial plate boundary between Arabia and Nubia. It connected the more evolved southern Red Sea mid-ocean ridge to the initially dominant Sirhan Rift. During this time, the MMTZ served as a primary lithospheric-scale boundary between the Arabia and Nubia plates. The Sirhan Rift and the MMTZ connection to the Red Sea spreading center was mostly abandoned with the development of the Dead Sea fault, and localization of extension in the present-day northern Red Sea. The transition to the present tectonic setting suggests an ephemeral rift–rift–transform triple junction within the central Red Sea connecting the localized southern Red Sea rift, a developing northern Red Sea rift, and the MMTZ transform.

## Introduction

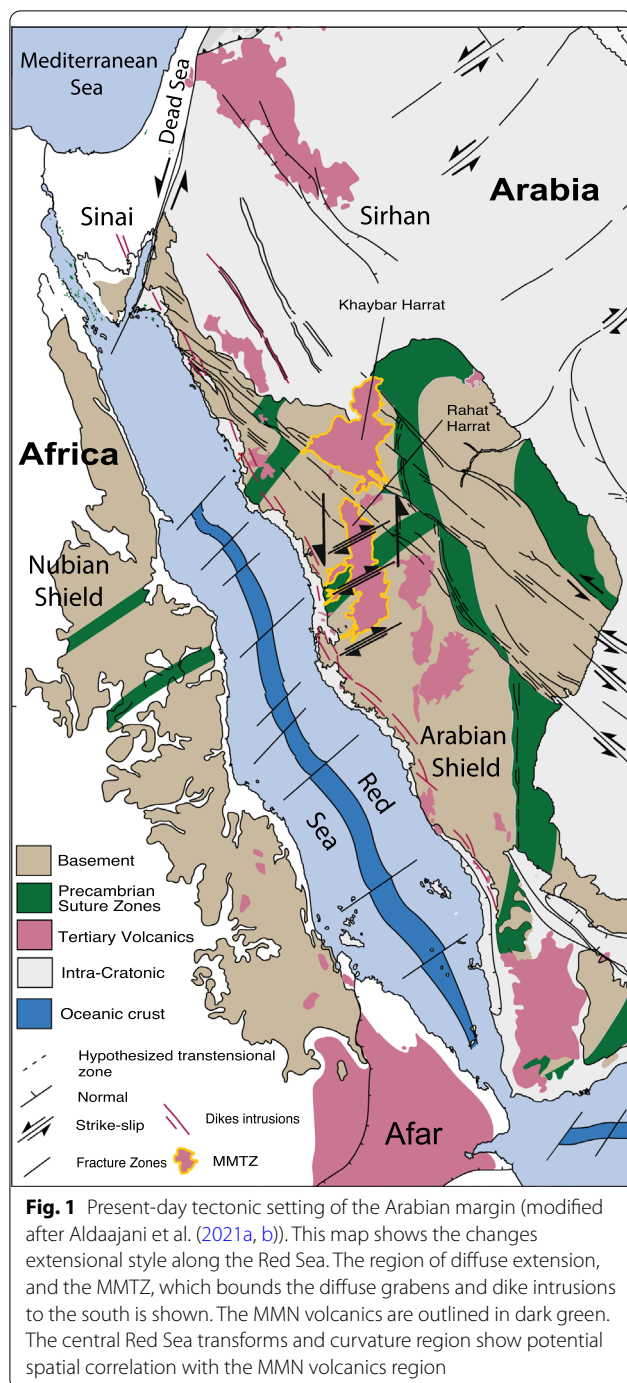
During the early stages of continental breakup, prior to the development of a fully formed mid-ocean ridge, a broad zone of extension may form (e.g., Wilson and Guiraud 1992). In some cases, the specific rift segments that evolve into the successful localized spreading centers may be significantly offset from each other, producing a continental rift–transform–rift structure that, with continued extension, may evolve into a large-offset ridge–transform–ridge structure such as the Romanche transform (e.g., Bonatti et al. 1995). Over time, with continued seafloor spreading, the two sides of the continental lithosphere bounding this initial transform become displaced from each other, complicating attempts to

document the processes associated with formation and initial motion along the transform (e.g., Swanson 1982).

The early Red Sea rift is characterized by differing southern localized (Almalki et al. 2015) and northern diffuse extensional styles (Roobol and Stewart 2009) (Fig. 1), with the northern diffuse extension considered to involve relatively symmetrical crustal stretching (Hosny and Nyblade 2016). The region of northern Red Sea (NRS) diffuse extension extends beyond the Red Sea itself, and is seen in the form of dikes, grabens, and ongoing volcanism outside the rift zone. The NRS extensional zone is bounded to the east by the Sirhan Rift (Roobol and Stewart 2009), to the west by the Egyptian western desert (Stockli and Bosworth 2019), to the north by the Mediterranean oceanic lithosphere (Erduran et al. 2008), and to the south by a localized volcanic activities along a lineament termed the Makkah–Madinah–Nafud (MMN) volcanic line (Camp and Roobol 1992). It should be noted that the extension rates today in this broad zone, outside

\*Correspondence: totaibi@kacst.edu.sa

<sup>1</sup> Department of Geosciences, Pennsylvania State University, 542 Deike Building, University Park, PA 16802, USA  
Full list of author information is available at the end of the article



the main NRS rift, are low (Aldaajani et al. 2021a, b). This region of diffuse extension predates the MMN volcanic line, since the region includes older diffuse grabens and dike intrusions (Roobol and Stewart 2009). In this paper, we call the structure bounding this extensional region on the south the Makkah–Madinah Transform Zone (MMTZ). This lithospheric-scale structure, across western Arabia, appears to have been initiated at ~30–28 Ma

based on the volcanic activities along two active rifting margins, the southern Red Sea (SRS) and the Sirhan rift.

The MMTZ and Sirhan were abandoned contemporaneously (23 Ma) with a major dike-intrusion event (Boone et al. 2021) along the Red Sea. Because of this abandonment, the MMTZ has preserved many of the characteristics of an early-stage rift-to-rift continental transform. Its tectonic activity since abandonment provides additional insight into the nature of an early stage lithospheric-scale plate boundary structure. Here we describe the evidence supporting this model of plate boundary evolution, test the process numerically using finite element methods, and discuss some of the insights into early-stage plate boundary formation provided by the MMTZ.

### Arabian Margin

The Arabian Margin (Fig. 1) has undergone extensive volcanism. Pre-rift volcanism in the vicinity of the Afar commenced at ~40 Ma, with maximum eruption rates at 30 Ma when rifting initiated (Wolfenden et al. 2005; Uksins et al. 2002). Volcanism began along the Sirhan rift at 28 Ma and continued until 22 Ma (Segev et al. 2014); it began along the SRS at ~28 Ma with activity continuing until 15 Ma (Bosworth and Stockli 2016). The petrology of volcanism along the SRS, the NRS and in the vicinity of the MMTZ supports the model of passive rifting for the Red Sea; (Konrad et al. 2016) and minimizes the influence of an Afar plume; although, several authors have argued for Afar plume importance for western Arabia volcanism based on geochemical constraints (e.g., Murcia et al. 2013). In general, the spatial variation of magmatic and structural architecture along the Red Sea rift suggests a combination of driving forces: slab pull and basal drag from a mantle plume (Aldaajani et al. 2021a, b). The temporal thermal evolution of the Red Sea suggests that there could have been a changing importance among mantle plume, plate boundary, and far field forces throughout the evolution of the Red Sea rift (Boone et al. 2021).

While the SRS rift is seen as an example of a magma rich margin associated with a narrow continental-rifting system (Fig. 1), the NRS rift during its initial period of early diffuse extension is considered to be hyperextended crust incorporating a magma poor margin (Stockli and Bosworth 2019; Blanchette et al. 2020) with diffuse extension (Roobol and Stewart 2009). The observed total extension over the diffuse extension region is 35 km (Steckler and ten Brink 1986; Bosworth et al. 2005) with regional stretching factor of 1.6 reported in the south of Suez rift (Gaulier et al. 1988) and likely in the northern Red Sea resulting in a reduction in crustal thickness of 10–15 km at ~15 Ma (Stockli and Bosworth 2019). This

extensional pattern in the NRS takes the form of parallel grabens and normal faults spread out within the north-western Arabian margin (Fig. 1). The history of diffuse extension is also preserved in dike intrusions (Fig. 1) along the NRS (Roobol and Stewart 2009). These pre-NRS localization grabens and dike intrusions are dated at 20–25 Ma, and appear to be bounded on the south by a tectonic structure that coincides with the present-day MMN volcanic line.

### Regional tectonics

The motion of Arabia with respect to stable Eurasia as inferred from broad-scale plate reconstructions and the extrapolation of geodetic measurements has been relatively constant for the last 30 Ma (McQuarrie et al. 2003; ArRajehi et al. 2010). Both geological and geodetic analysis estimate 20 km/Ma displacement of Arabia with respect to Eurasia. The Arabia–Eurasia collision along the Zagros mountains (to the east) formed with the closure of the Neo-Tethys ocean at ~27 Ma (Pirouz et al. 2017). The motion of Nubia with respect to Eurasia changed significantly throughout the Miocene having decreased three times, at 30, 24, and ~13 Ma. The first decrease occurred at ~30 Ma contemporaneous with Aegean basin formation (Jolivet and Faccenna 2000), the initiation of Nubian slab roll-back under the eastern Mediterranean region (Agostini et al. 2010), and initiation of the Nile River (Faccenna et al. 2019). The second decrease occurred at ~24 Ma contemporaneous with rapid cooling in the southern segment of the Dead Sea Transform (Morag et al. 2019) and initial localization of the Red Sea rifting (Reilinger and McClusky 2011), as reported rates are equal within uncertainties for Arabia and Nubia. The third decrease occurred at ~13 Ma leading to a 70% increase in Arabia–Nubia plate motion (ArRajehi et al. 2010), within uncertainties equal to geologic estimates. This is contemporaneous with an uplift along the Arabian margin (Bohannon et al. 1989), suggesting a potential correlation with the onset of MMTZ volcanism. Widely spaced in time reconstructions of the history of convergence between the Nubia and Eurasia plates before 20 Ma, and the 1 cm/year Nubia–Eurasia plate motion estimate for the last 20 Ma, complicate the plate motion estimate and its precision, respectively (DeMets et al. 2015).

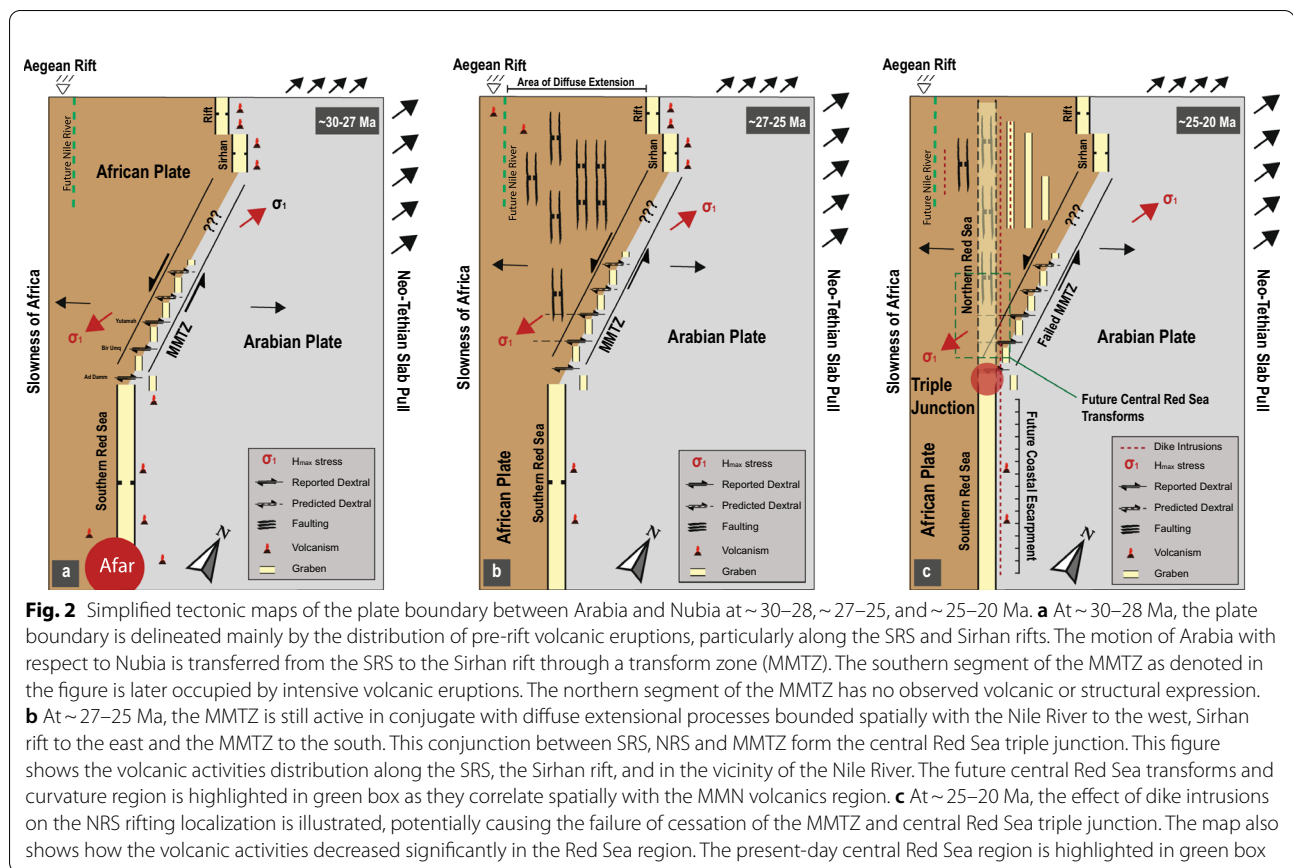
Following the Afar thermal (heating) event, two cooling events are interpreted to have occurred between 25–20 Ma and at ~15–13 Ma in the SRS rift (Bohannon et al. 1989) and in the central Red Sea (Szymenski et al. 2016). In contrast, a single cooling event was reported in the vicinity of the Dead Sea Transform between 25–18 Ma (Morag et al. 2019). An earlier cooling event occurred in the Gulf of Aden rift at ~33 Ma (Leroy et al.

2012). The onset of NRS rifting is inferred to have begun during the Oligocene based on a crustal cooling event (i.e., exhumation) in the northern segment (Omar and Steckler 1995) and the seismic stratigraphy of the north-western Arabian margin (Tubbs et al. 2014). Results of apatite fission track analyses from the Neo-Proterozoic basement in the eastern desert of Egypt also indicate an Oligocene start for a cooling event (Bojar et al. 2002).

The Dead Sea Transform formed at ~20 Ma (Nuriel et al. 2017), or younger at 17 Ma (Kohn et al. 2019), soon after the dike-intrusion event along the Red Sea (Boone et al. 2021) providing a pathway to eventually abandon the MMTZ–Sirhan rift plate boundary system. The development of the Dead Sea Transform most likely played an important role in the demise of the Sirhan rift and changing the extensional style along the Red Sea from orthogonal to oblique (Segev et al. 2017). Apatite fission track analyses from the Arabian shield in Jordan also record an Oligocene cooling event, although these samples are located 200 km away from the Red Sea rift (Feinstein et al. 2013). This extensive cooling event, within the northwestern Arabian margin is in contrast to an inferred steady-state geotherm along the central Arabian margin, based on fission track data (Szymenski et al. 2016).

### Proposed tectonics

We follow a chronological order to describe the tectonic activities in the Mediterranean–Red Sea region. In our model, this tectonism began with the initiation of Nubia slab roll-back, producing the Aegean basin around 30 Ma. This event is associated with the reduction of Nubia northward motion with respect to the Eurasian plate, as shown schematically in Fig. 2a. This was contemporaneous with rifting along both the Sirhan and the SRS rifts. We infer that the northward motion of the eastern Mediterranean block, in the vicinity of the Aegean rift, ceased, transferring plate motion between the SRS rift and the Sirhan rift, within the Arabian margin. Both rifts were active and magma rich at this time. This change in motion drove the formation of the plate boundary between Arabia and Nubia around 30–28 Ma, which served as the initial plate boundary structure in the region as Arabia separated from Nubia. This plate boundary emerged as sinistral transtensional zone segmented by multiple dextral strike–slips, including Ad Damm, Bir Umq (Stern and Johnson 2019), and Al-Yutamah shear zones (Bamoussa 2013) (Fig. 2). The duration of the MMTZ as a primary plate boundary structure is relatively short, less than 5 Ma, as the NRS soon developed and began to accommodate a majority of the lithospheric extension—leading to a decrease in activity in the Sirhan Rift and along the MMTZ. During this



transition time, these conjugate structures (SRS–NRS–MMTZ) form a rift–rift–transform triple junction that we call here the central Red Sea triple junction. This triple junction appears to have been ephemeral also existing for less than 5 Ma.

The NRS started developing graben structures across a wide domain between ~27 and ~25 Ma (Fig. 2b). The extension in the NRS is likely driven by far field forces, either from the collision between Arabia–Eurasia or the relative acceleration of the eastern Mediterranean, to the east of Aegean rift, with the respect to slab roll-back beneath the Aegean rift (Fig. 5). We incorporate the tectonic effects of the central Red Sea triple junction into our modeling by introducing kinematic boundary conditions (defining displacement) instead of slippery nodes (allowing displacement) along the SRS (Fig. 6). The resulting strain localizes along the present NRS in the form of localized extension by ~25 Ma (Figs. 2c, 6), that is then occupied by the succeeding dike intrusions at 24–23 Ma. The spatial extent of decompression melting and the implications for dynamics remain uncertain (Wright et al. 2012). These dikes may have developed due to the northward propagation of lithospheric thinning (Mondy et al. 2018; Buck 2006) from the SRS to the

NRS, a regional change in the stress field caused by the slab roll-back in the Mediterranean (Figs. 2b, 5), or in response to early oblique extensional forces (Brune et al. 2018) driven by the Arabia–Eurasia collision onset.

## Methods

To better understand what may have initiated the evolution of the MMTZ, we evaluate the role that regional tectonic forces acting on western Arabia could have in initiating and/or driving this deformation. Determining the possible underlying causes of this process are a key part of resolving many of the regional geodynamic problems including the driver for the formation of the central and northern Red Sea. In this section, we use the finite element approach to test the effect of three potential tectonic settings that may describe the underlying processes of the proposed tectonics outlined in Fig. 2a–c. The boundary conditions for each model satisfy the published constraints on the Afro-Arabia plate boundaries, in particular within the Mediterranean, and along the Red Sea, the Gulf of Aden and the Sirhan. We test the effect of these boundary conditions on the strain rate patterns within the Arabian margin. The resulting strain patterns provide an insight into the underlying mechanisms of the



MMTZ formation, extensional changes and off-axis dike intrusions along the Red Sea, and the potential role of regional tectonic forces, in particular with the Mediterranean, on the Red Sea and Arabian margin evolution.

We model the effects of tectonic forces acting along the Afro-Arabian plate boundaries between 30–20 Ma to test their sensitivity on this proposed tectonic evolution of the Arabian margin and the Red Sea rift. We define our model domain and constraints to test this tectonic process in light of the tectonic forces described in “Arabian margin” Section. Our goal is to utilize the kinematic evolution of the Afro-Arabia plate edges in the form of boundary and slippery node conditions to test the sensitivity of these conditions to the resulting strain rate patterns within the Arabian margin during various geological time frames. To achieve our goal, we develop a numerical deformational model for the Afro-Arabia

Plate system, including our area of interest (Fig. 3, inset A). The large-scale regional tectonic forces acting on the Arabian margin area at this time are Neo-Tethys slab pull, Nubian slab roll-back, and possibly other mantle related processes (i.e., Afar plume or other mantle flow). We focus our investigation on the interaction between the Neo-Tethys slab pull and Nubian slab roll-back forces and their effects in activating pre-existing structures and weaknesses within the Arabian margin.

### Model setting

The model domain is a two-dimensional plane-stress spherical shell, which is assumed to be thin in the vertical direction. We use the GTECTON platform (version 2017.3; Govers and Wortel 1993; Govers and Meijer 2001; Özbakir et al. 2017) to compute velocity, stress ( $\sigma$ ) and strain ( $\epsilon$ ) rates by solving the mechanical

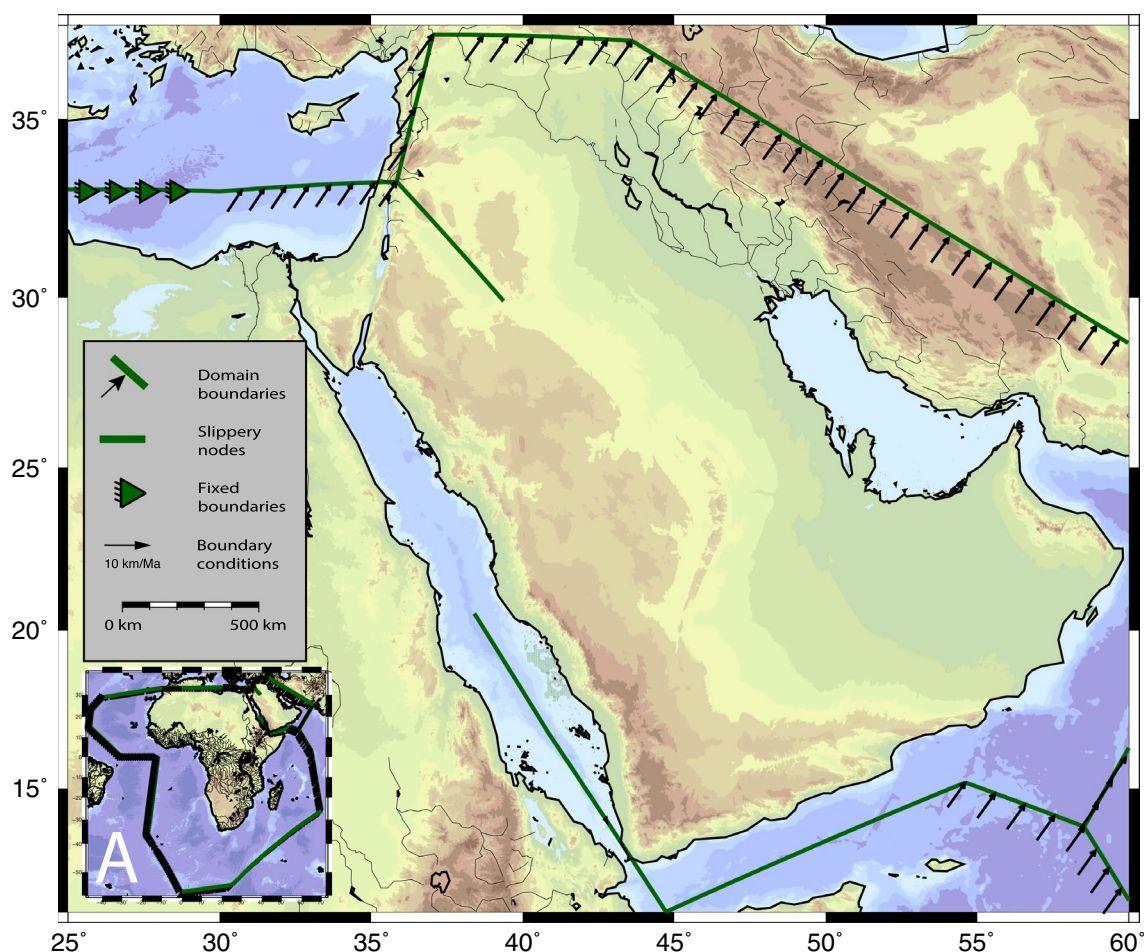


**Fig. 3** Deformational model domain. This map shows the model domain for the Afro-Arabia plate system at 30–28 Ma. Because of this, the northern boundary of our domain does not coincide with the present geographic outlines for Nubia. The black arrows represent our boundary conditions with stable Eurasia reference frame. The green triangles denote our fixed boundaries. The green lines are assigned with slippery node conditions. The insert shows the whole model domain where we apply our boundary conditions and calculate the resulted strain rate field

equilibrium equations. The GTECTON platform assumes that each individual element is a thin plane, and all of them are connected together to describe the outline of a spherical shell. This allows the use of a planar cartesian description of the mechanical equilibrium equations. We represent the model domain by a homogeneous elastic material (Young's modulus = 7.5 GPa; Poisson's ratio = 0.30) with discrete faults and a triangular element mesh. Our model does not depend on temperature nor time; rather, it represents the corresponding kinematic boundary conditions in a particular time. The constraints on the plate boundary kinematics have been approximated mainly from relative Afro-Arabia plate motion with respect to the Eurasian plate.

In our model (Fig. 3), we fix the western edge and the Aegean block, which is part of the eastern Mediterranean, and assign velocity boundary conditions along the northern and eastern edges, including the rest of eastern Mediterranean, Anatolia, Zagros, Makran, and along the boundary between Nubian and Indian plate. We introduce slippery node structures, with two degrees of freedom, within the Afro-Arabia plate in the southern Red Sea, Gulf of Aden, and Sirhan rift. The slippery node conditions allow passive rifting activities along these structures, by which the extensional processes will be driven by far field forces. The strain rate will be very low in the vicinity of the slippery node structures as the displacement is mainly accommodated along the faults. This approximation is valid as we focus on the regional forces rather than local processes.

We assign 20 km/Ma velocity boundary condition along the eastern boundary on the Arabian plate (Fig. 3), with 95% confidence uncertainties as extrapolated by geodetic measurements (ArRajehi et al. 2010). We use late circuit closures based on magnetic seafloor anomalies and geological reconstructions of crustal shortening in Iran (McQuarrie et al. 2003) to estimate convergence rate along Arabia–Eurasia at 20 km/Ma with uncertainty ellipses representing 95% confidence (Molnar and Stock 1985). Along the Nubia–Eurasia plate boundary, we assign 5 km/Ma velocity boundary condition as extrapolated from DeMets et al. (2010) based on reconstructions of the history of convergence between the Nubia and Eurasia plates. We set this constant value for the plate boundary kinematics as we are interested to highlight the first order sensitivity to the differences between plate boundaries (Arabia–Eurasia versus Nubia–Eurasia) rather than the differences within a single plate boundary due to plate rotation.

## Results

As we are interested in the strain patterns within the Arabian margin region, the effects of abrupt or step changes in boundary conditions along the northern boundary region of our domain, which is ~500 km away from the area of interest, have a minimal impact on our results. Nevertheless, we use a coarse mesh to smooth and minimize any potential effects, resulting from edges or jumps in the velocity boundary conditions, to our region of interest. Our results are sensitive to the nature of boundary conditions along the Mediterranean and the southern segment of the Red Sea, in particular the slippery nodes and kinematic conditions. To assess this sensitivity, we test three scenarios. In the first scenario, we impose passive rifting along Sirhan, southern Red Sea, and Gulf of Aden rifts with fixing the Aegean rift and eastern Mediterranean. While in the second scenario, we use the same setting as in the first scenario with introducing kinematic boundary conditions to the eastern Mediterranean. Last, in the third scenario we test both settings as in the first and second scenarios with introducing a motion along the southern Red Sea and Gulf of Aden rifts.

The spatial distribution of the early volcanism (~30–28 Ma) suggests tectonic activities along the southern Red Sea and Sirhan rifts (Wolfenden et al. 2005; Uksutins et al. 2002). In the first scenario, we assign slippery node conditions along the southern Red Sea and Sirhan, fix the Aegean block, and reduce the velocity along the eastern Mediterranean block (Fig. 4). The resulting strain localizes along a zone that links the northern tip of the southern Red Sea to the Sirhan rift. This zone exhibits a combination of dilatational strain with sinistral strike-slip motion, i.e., a transtensional strain zone. This occurs because of the differential motion between the southern Red Sea and Sirhan rifts. The dilatational strain rate magnitude (Fig. 4) ranges between 0.02–0.1 strain per million years. Although there are high strain rate concentrations around the edges of the slippery nodes that is a likely a local edge effect at the tips of the defined structures. Nevertheless, the regional dilatational strain rate pattern produces a pathway to transfer the deformation from the southern Red Sea rift to the Sirhan rift. This transtensional strain rate pattern appears to be controlled by regional forces, such as the slowing of the Nubian plate that are associated with the onset of Aegean extension due to the Nubian slab roll-back, and passive rifting along the southern Red Sea and Sirhan.

We also tested the potential effect of accelerating the eastern (Fig. 5) Mediterranean block. Hence, in our second set of models we assign slippery node conditions along the southern Red Sea, fix the Aegean block, and accelerate the velocity along the eastern Mediterranean block. The resulting dilatational strain rate

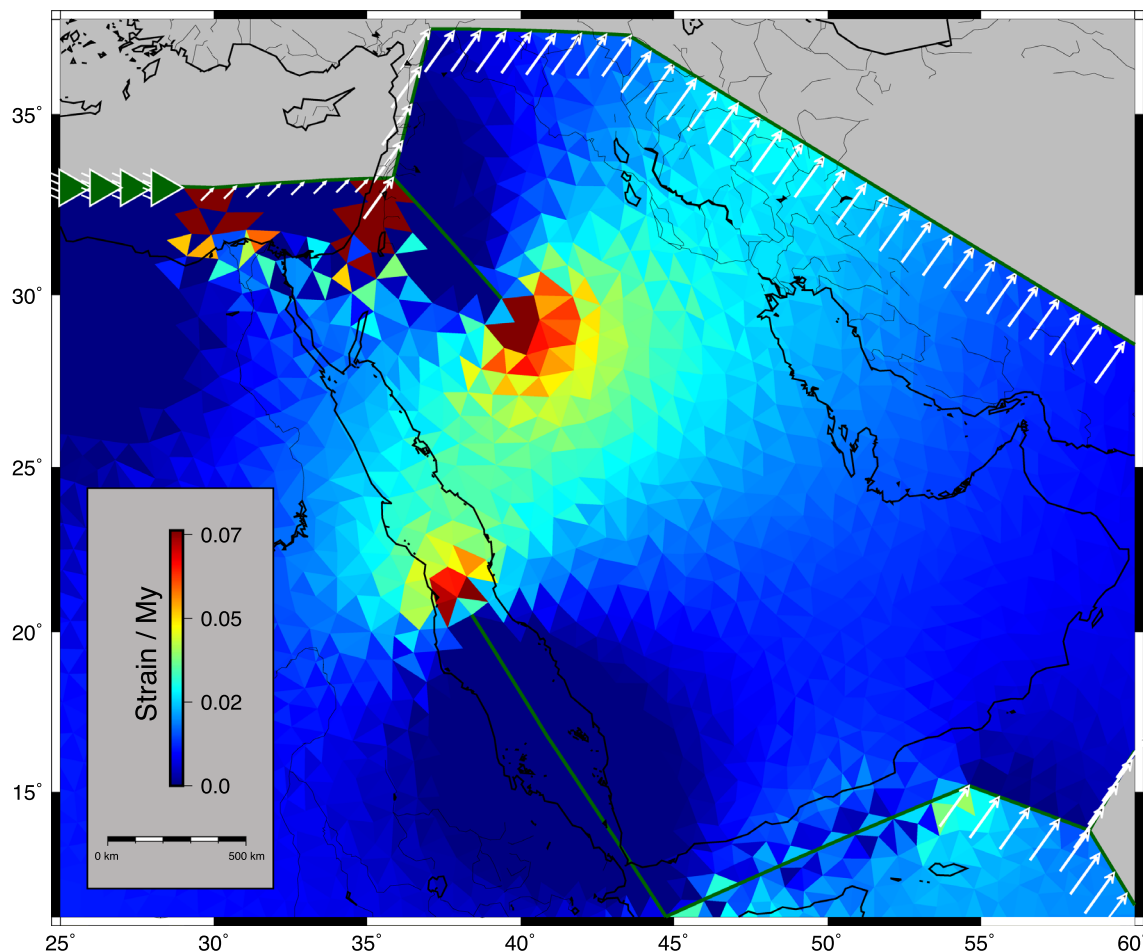


**Fig. 4** Strain rate map of the Arabian margin around 30–28 Ma. The dilatational strain rate localizes along a transform zone that produced by the differential motion between the SRS and the Sirhan rifts. We hypothesize that this strain rate pattern was driven by the slowing along the northern boundary, which caused by the onset of Aegean rift due to the Nubian slab roll-back, and passive rifting along the RS and the Sirhan. Along our defined slippery nodes the strain is very low as the displacement occurred mainly along the faults. We using oversimplified rheology as we intend here to highlight a first order process as a function of the given regional boundary conditions, where the region of interest is either covered by volcanic lavas or sand dunes. Although the strain rate pattern covers the whole region between the SRS and Sirhan rift, the volcanic eruptions are observed only in the southern segment of the MMTZ

(Fig. 5) suggests a wide extensional zone within the northern Red Sea region. This zone, which can be seen in our model Fig. 5, is bounded by the Egyptian western desert to west, the Sirhan rift to the east, the MMTZ to the south, and the eastern Mediterranean to the north. At the time the southern Red Sea rift becomes a more localized plate boundary (~25–23 Ma), the volcanism along the Sirhan rift ceases (~23 Ma) while the northern Red Sea is still undergoing diffuse rifting (Stockli and Bosworth 2019). This observation led us to our third model, where we assign kinematic conditions along the southern Red Sea and Gulf of Aden, fix the Aegean block, and increase the velocity along the eastern Mediterranean block (Fig. 6).

In general, we find that the resulting strain rate patterns from our modeling are sensitive to the boundary conditions along the southern Red Sea and Gulf of Aden. Introducing specific kinematic conditions along the southern Red Sea localizes the deformation along the northern Red Sea. Moreover, the resulting pattern of regional strain is also sensitive to the structural geometries appropriate for the southern Red Sea and Sirhan rifts.

### Discussion

Our hypothesis is that the MMTZ is a short-lived leaky, rift-to-rift continental transform that had become a relict plate boundary prior to the emplacement of the more



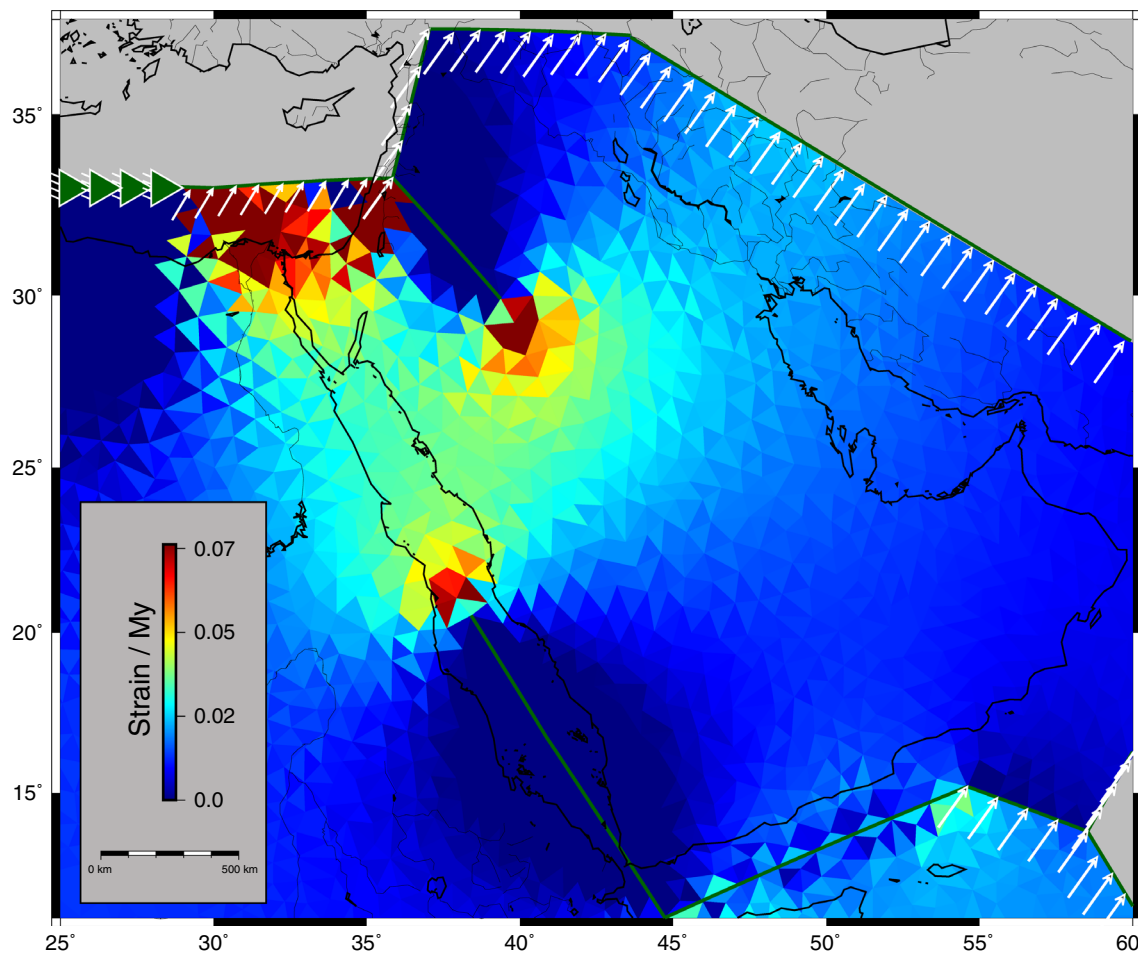


**Fig. 5** Strain rate map that correspond to the increase of velocity in the eastern Mediterranean with keeping the rest of the boundary conditions as described in Fig. 3. This process demonstrates that during the period between development of the Nile River zone (30–28 Ma) until the dike intrusions event (25 Ma) hyperextension was taking place along the NRS, and dilatational strain rate diffuses from the Egyptian western dessert to the Sirhan rift. Although the deformation becomes more diffuse in comparison with Fig. 4, the strain zone linking the SRS and the Sirhan rifts still bounds the diffuse extension area to the south. For simplicity, we use a homogenous elastic domains in which the dilatational strain tends to be uniformly distributed

recent MMN volcanics, within the western Arabian margin. This model for the MMTZ formation is in general agreement with a previous suggestion of Camp and Roobol (1992), who concluded there was sinistral strike-slip motion along the MMTZ (what they called the MMN volcanic line). Their interpretation was based on two main observations, the en echelon spatial distribution of late-Miocene volcanic cone segments along the MMTZ, and counterclockwise block rotation based on paleomagnetic data. The amount of shear and extension that can occur along the MMTZ is constrained by the time between the slowdown of Nubia with respect to Eurasia and the Red Sea dike-intrusion event.

Previously the MMTZ has been linked to asthenospheric upwelling processes (Szymanski et al. 2016),

who attributed the diffuse extension to a decoupling between an asthenosphere channel beneath the volcanic line and lithosphere. This asthenosphere channel was assumed to be a long-lived structure formed during the early Paleozoic (Coleman 1974). However, a more recent crustal thickness map of the Arabian plate (Blanchette et al. 2020) shows no significant crustal thickness variation across the MMTZ region implying negligible crustal growth associated with the MMTZ volcanism. This suggests that the MMTZ structure is relatively recent. Moreover, evidence from seismic reflection profiles across the northern extent of the MMTZ, within the northwestern Arabian basin, cast doubt on it being a long-lived structure (Khalil, 2016). The lack of evidence for an older (Paleozoic) initiation supports our interpretation that the



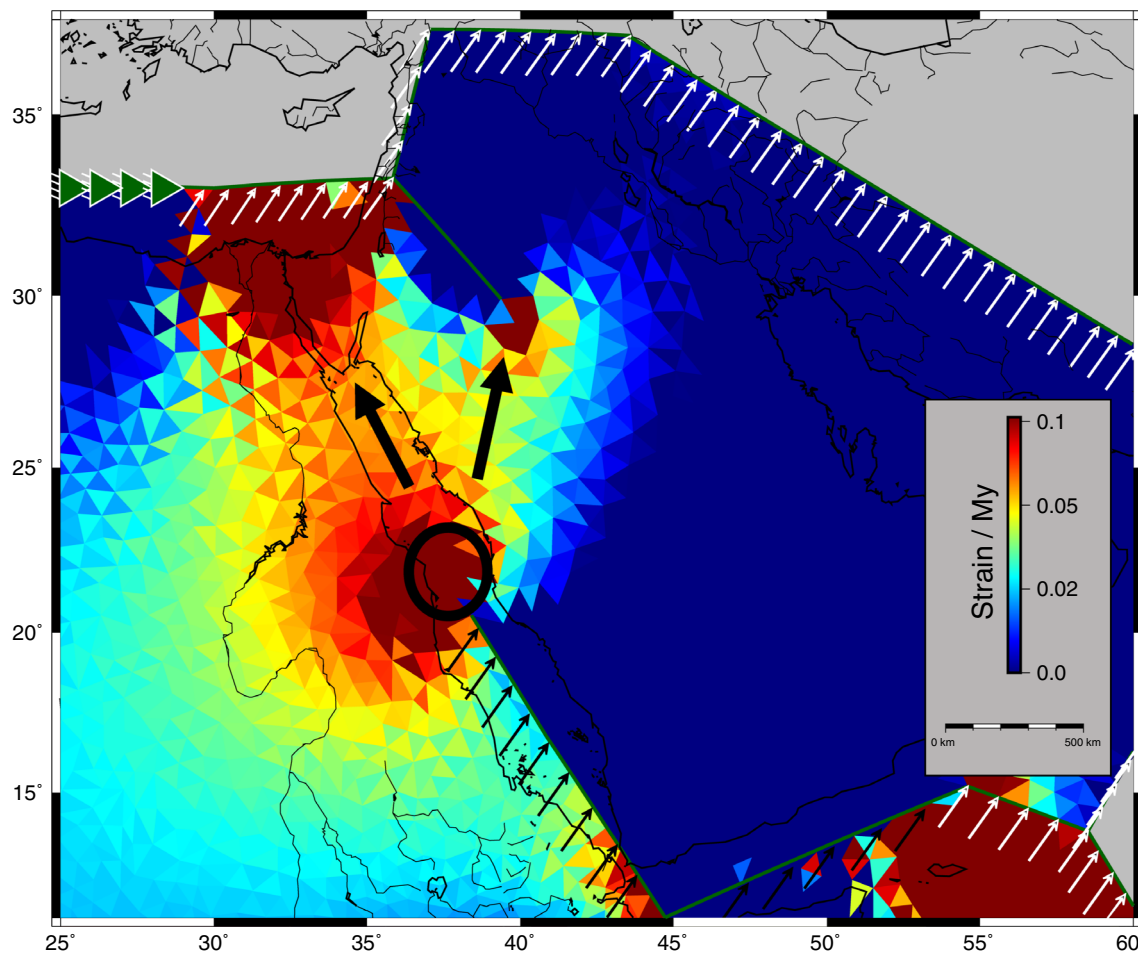


**Fig. 6** Strain rate map that correspond to the change of the SRS and Gulf of Aden kinematic conditions (black arrows). The strain distribution here reflects the boundary conditions corresponding to the time interval between initiation of dike intrusion along the Red Sea (24 Ma) until the development of the Dead Sea Transform (20 Ma). The dilatational strain rate localizes along the NRS. For simplicity, we are using a homogeneous elastic domain in which the dilatational strain tends to be uniformly distributed. The black circle highlights the location of the hypothesized central RS triple junction. The black arrows represent the northern two arms, the MMTZ transform and NRS rift

MMTZ likely formed more recently in the Cenozoic, and should be explained in light of the more recent pattern and evolution of tectonic forces acting on the Arabian plate boundaries, since the Oligocene.

Our results imply that the MMTZ, as nascent plate boundary, formed by connecting the northern tip of the SRS localized extension ( $\sim 21^\circ$  latitude), with the southern tip of Sirhan rift. The south-western segment of the MMTZ shows good alignment with the spatial distribution of the more recent MMN volcanics (Fig. 1), while the north-eastern segment (Fig. 2a) of the MMTZ extends beyond the MMN volcanics. Tertiary basalts have been reported in the vicinity of Madinah city (Bamousa 2013), which support the interpretation of activity along of the MMTZ prior to the NRS initiation. We envision the MMTZ as transtensional zone with sinistral strike-slip motion as inferred from our

numerical results (Fig. 4). While the sinistral strike-slip is function of regional forces, the absence of dextral strike-slip in our numerical results (Figs. 4, 5, and 6) demonstrate the importance of either increasing the rheological complexity in our model setting, accounting the plate rotation effect by varying the velocity boundary conditions along the plate boundaries, or introducing inherited weaknesses within the Arabian margin. We suggest that the northern MMTZ, which does not have an obvious surface manifestation, is either currently covered by the Great Nafud sand dunes, or may have had a more subtle surface structural expression. In brief, this proposal that the MMTZ is a relict plate boundary that was active prior to plate boundary localization along the NRS provides a framework to investigate the spatial and temporal evolution of the Red Sea and western Arabian margin and provides insights into

how the early stages of continental-rifting to seafloor spreading evolve.

The dike intrusions along the Red Sea represent a regional tectono-magmatic event associated either with oblique plate motion, which may lead to regional changes in stress and therefore facilitate strain localization (Brune et al. 2018) or by a northward propagation of the asthenosphere (Mondy et al. 2018) which may lead to thinning (Buck 2006). Here we lean toward the importance of obliquity in forming the structural pattern seen along the Red Sea, with the role of asthenospheric propagation primarily to produce dike intrusions within pre-existing rift related structures.

The central Red Sea curvature and transforms correlate well with the southern MMTZ, and may have developed as a natural response to the early competition between extension on the MMTZ and northward propagation of the Red Sea. We call this tectonic arrangement the central Red Sea triple junction, which connects the SRS, NRS, and MMTZ. We tested multiple boundary conditions (“Discussion” Section) to produce this tectonic setting, and we find the kinematic condition along the SRS can favor the development of the NRS and failure of the MMTZ. The resulting dilatational strain rate with these kinematic conditions (Fig. 6) suggests the localization of strain along the NRS instead of MMTZ. The transition process from the MMTZ to NRS leads to the development of the central Red Sea triple junction. Hence, we hypothesize that the present-day central Red Sea architecture is resulted from an early competition between the NRS and MMTZ.

Volcanism along the MMTZ commenced at 13 Ma (Boone et al. 2021), contemporary with the last phase of Nubia–Eurasia slowing (Reilinger and McClusky 2011). This slowing event may have led to another episode of sinistral strike–slip motion along the MMTZ, producing volcanism and adding extra shear into the MMTZ inherited structures. This can be inferred in the dextral strike–slip faults that correlated with major stepping over of the volcanic cones lineament (Downs et al. 2018) within the Rahat Harrat (Fig. 1), as the observed trend of these dextral faults is N60 (Bamoussa 2013), which suggests an active sinistral shearing along the southern segment of the MMTZ. However, the lack of data to map the dextral strike–slip faults in the vicinity of the Khaybar Harrat (Fig. 1) calls for further investigation.

## Conclusion

The initiation of the Red Sea rift has been reported by many researchers to occur between 30–20 Ma based on a broad spectrum of field data, meanwhile, its evolution involved several rifting stages observed

on the Arabian margin in the form of dike intrusions, volcanic eruptions and uplift events. Since the 1980s, many researchers have suggested that there is a link between these tectonic activities and the regional tectonic forces; however, very few numerical models have previously been developed (e.g., Artemieva et al. 2022). Hence, in this work, we are using the finite element modeling approach to highlight the mechanical deformation processes driving Red Sea rifting initiation and evolution as a function of the regional tectonic forces.

Our finite element models implement the kinematic evolution of the Afro-Arabia plate edges in the form of boundary and slippery nodes conditions to test the sensitivity of these conditions for predicted strain patterns along the Red Sea and within the Arabian margin during various geological time frames. Our results show that the motion among northern Africa with respect to Eurasian plate played an important role on the MMTZ formation and the northern Red Sea diffuse extension processes. Evolution of the southern Red Sea was the driving mechanism for the northern Red Sea formation. In detail, the MMTZ formed by transferring the motion from the southern Red Sea to Sirhan rift which initiated due to a slowing Nubia with respect to Eurasia as a result of the Nubian slab roll-back in the Mediterranean. By introducing slippery node conditions along the southern Red and Gulf of Aden the resulting stresses along the northern Red Sea are amplified and promote the northward propagation of the rift system. By propagating the Red Sea rift northward, the central Red Sea transforms become a natural response to the early competition between the MMTZ and northward propagation processes. This competing process may reduce the strain rates magnitudes under the needed threshold to localize the central Red Sea rift.

## Acknowledgements

We acknowledge the King Abdulaziz City for Science and Technology (KACST) for supporting this research. Thamer Aldaajani is supported by KACST, and Kevin Furlong is supported by the Pennsylvania State University- University Park. Many of the figures were produced using GMT (Wessel and Smith, 1991).

## Author contributions

Both authors have made a substantial, direct, and intellectual contribution to the work and approved it for publication. Both authors read and approved the final manuscript.

## Funding

No fund provided.

## Availability of data and materials

Not applicable.

## Declarations

## Competing interests

The authors declare that they have no competing interests.

**Author details**

<sup>1</sup>Department of Geosciences, Pennsylvania State University, 542 Deike Building, University Park, PA 16802, USA. <sup>2</sup>King Abdulaziz City for Science and Technology, Riyadh 11442, Saudi Arabia.

Received: 8 August 2021 Accepted: 15 April 2022

Published online: 12 May 2022

**References**

- Agostini S, Doglioni C, Innocenti F, Manetti P, Tonarini S (2010) On the geodynamics of the Aegean rift. *Tectonophysics* 488(1–4):7–21
- Aldaajani TZ, Almalki KA, Betts PG (2021a) Plume Versus Slab-Pull: example from the Arabian Plate. *Front Earth Sci* 9:494
- Aldaajani T, Furlong K, Malservisi R (2021b) The rigidity of the western Arabian margin: extensional strain rate field from GPS networks. *Arab J Geosci* 14(5):1–11
- Almalki KA, Betts PG, Ailleres L (2015) The Red Sea—50 years of geological and geophysical research. *Earth Sci Rev* 147:109–140
- ArRajehi A, McClusky S, Reilinger R, Daoud M, Alchalbi A, Francisco G, Ergintav S et al (2010) Geodetic constraints on present-day motion of the Arabian Plate: implications for Red Sea and Gulf of Aden rifting. *Tectonics*. <https://doi.org/10.1029/2009TC002482>
- Artemieva IM, Yang H, Thybo H (2022) Incipient ocean spreading beneath the Arabian shield. *Earth-Sci Rev*. <https://doi.org/10.1016/j.earscirev.2022.103955>
- Bamoussa AO (2013) Complex tectonic history of Al-Yutamah dome area within Hijaz Terrane, Arabian Shield, South of Al Madinah, Saudi Arabia. *Open Geol J*. <https://doi.org/10.2174/1874262920130806002>
- Bamoussa AO, Matar SS, Daoudi M, Al-Doaan MI (2013) Structural and geomorphic features accommodating groundwater of Al-Madinah City Saudi Arabia. *Arabian J Geosci*. <https://doi.org/10.1007/s12517-012-0574-x>
- Blanchette A, Klemperer S, Mooney W, Zahran H (2020) Thickness of the Saudi Arabian Crust. *EarthArXiv*. <https://doi.org/10.31223/X5CP47>
- Bohannon RG, Naeser CW, Schmidt DL, Zimmermann RA (1989) The timing of uplift, volcanism, and rifting peripheral to the Red Sea: a case for passive rifting? *J Geophys Res*. <https://doi.org/10.1029/JB094iB02p01683>
- Bojar A-V, Fritz H, Kargl S, Unzog W (2002) Phanerozoic tectonothermal history of the Arabian-Nubian shield in the Eastern Desert of Egypt: evidence from fission track and paleostress data. *J Nubian Earth Sci* 34(3–4):191–202
- Bonatti E, Ligi M, Gasperini L, Peyve A, Raznitsin Y, Chen YJ (1995) Transform migration and vertical tectonics at the Romanche Fracture Zone, equatorial Atlantic. *Oceanogr Lit Rev* 5(42):370
- Boone SC, Balestrieri M-L, Kohn B (2021) Thermo-tectonic imaging of the Gulf of Aden-Red Sea rift systems and Afro-Arabian hinterland. *Earth Sci Rev* 222:103824
- Bosworth W, Stockli DF (2016) Early magmatism in the greater Red Sea rift: timing and significance. *Can J Earth Sci* 1176(April):1–19. <https://doi.org/10.1139/cjes-2016-0019>
- Bosworth W, Huchon P, McClay K (2005) The Red Sea and gulf of Aden basins. *J Nubian Earth Sci* 43(1):334–378
- Brune S, Williams SE, Dietmar Müller R (2018) Oblique rifting: the rule, not the exception. *Solid Earth* 9:1187–1206. <https://doi.org/10.5194/se-9-1187-2018>
- Buck WR (2006) The role of magma in the development of the Afro-Arabian Rift System. *Geol Soc Lond Spec Pub* 259(1):43–54
- Camp VE, Roobol MJ (1992) Upwelling asthenosphere beneath western Arabia and its regional implications. *J Geophys Res* 97(B11):15255–15271
- Coleman RG (1974) Geologic background of the Red Sea. *The geology of continental margins*. Springer, Berlin, pp 743–751
- DeMets C, Gordon RG, Argus DF (2010) Geologically current plate motions. *Geophys J Int* 181(1):1–80
- DeMets C, Iaffaldano G, Merkuriev S (2015) High-resolution Neogene and quaternary estimates of Nubia-Eurasia-North America plate motion. *Geophys J Int* 203(1):416–427
- Downs DT, Stelten ME, Champion DE, Dietterich HR, Nawab Z, Zahran H, Hassan K, Shawali J (2018) Volcanic history of the northernmost part of the Harrat Rahat volcanic field, Saudi Arabia. *Geosphere* 14(3):1253–1282
- Erduran M, Endrun B, Meier T (2008) Continental vs. oceanic lithosphere beneath the eastern Mediterranean Sea—implications from Rayleigh wave dispersion measurements. *Tectonophysics* 457(1–2):42–52
- Faccenna C, Glišović P, Forte A, Becker TW, Garzanti E, Sembroni A, Gvirtzman Z (2019) Role of dynamic topography in sustaining the Nile River over 30 million years. *Nat Geosci* 12(12):1012–1017
- Feinstein S, Eyal M, Kohn BP, Steckler MS, Ibrahim KM, Moh'd BK, Tian Y (2013) Uplift and denudation history of the eastern Dead Sea rift flank, SW Jordan: evidence from apatite fission track thermochronometry. *Tectonics* 32(5):1513–1528
- Gaulier JM, Le Pichon X, Lyberis N, Avedik F, Geli L, Moretti I, Deschamps A, Hafez S (1988) Seismic study of the crust of the northern Red Sea and Gulf of Suez. *Tectonophysics*. [https://doi.org/10.1016/0040-1951\(88\)90007-8](https://doi.org/10.1016/0040-1951(88)90007-8)
- Govers R, Meijer PT (2001) On the dynamics of the Juan de Fuca plate. *Earth Planet Sci Lett* 189(3–4):115–131
- Govers R, Wortel MJR (1993) Initiation of asymmetric extension in continental lithosphere. *Tectonophysics* 223(1–2):75–96
- Hosny A, Nyblade A (2016) The crustal structure of Egypt and the northern Red Sea region. *Tectonophysics* 687:257–267
- Jolivet L, Faccenna C (2000) Mediterranean extension and the Africa-Eurasia collision. *Tectonics* 19(6):1095–1106
- Khalil M (2016) Control of Intra-Plate tectonic inversion on the East and North Saudi Arabia Basins. In: 12th Middle East Geosciences Conference & Exhibition. Bahrain, New Explor Horiz. 30458
- Kohn B, Weissbrod T, Chung L, Farley K, Bodorkos S (2019) Low-temperature thermochronology of francolite: insights into timing of Dead Sea transform motion. *Terra Nova* 31(3):205–219
- Konrad K, Graham DW, Thornber CR, Duncan RA, Kent AJR, Al-Amri AM (2016) Asthenosphere–lithosphere interactions in Western Saudi Arabia: inferences from 3He/4He in xenoliths and lava flows from Harrat Hutaymah. *Lithos* 248:339–352
- Leroy S, Razin P, Autin J, Bache F, d'Acremont E, Watremez L, Robinet J et al (2012) From rifting to oceanic spreading in the Gulf of Aden: a synthesis. *Arabian J Geosci* 5:859–901
- McQuarrie N, Stock JM, Verdel C, Wernicke BP (2003) Cenozoic evolution of Neotethys and implications for the causes of plate motions. *Geophys Res Lett*. <https://doi.org/10.1029/2003GL017992>
- Molnar P, Stock JM (1985) A method for bounding uncertainties in combined plate reconstructions. *J Geophys Res Solid Earth*. <https://doi.org/10.1029/JB090iB14p12537>
- Mondy LS, Rey PF, Duclaux G, Moresi L (2018) The role of asthenospheric flow during rift propagation and breakup. *Geology* 46(2):103–106
- Morag N, Haviv I, Eyal M, Kohn BP, Feinstein S (2019) Early flank uplift along the Suez Rift: implications for the role of mantle plumes and the onset of the Dead Sea transform. *Earth Planet Sci Lett* 516:56–65
- Murcia H, Lindsay JM, Niedermann S, Cronin SJ, Smith IEM, ElMasry NN, Moufti MRH, Németh K (2013) The potential use of cosmogenic nuclides for dating in Harrat Rahat. In: VORISA Scientific Meeting extended abstract. p. 24–28
- Nuriel P, Weinberger R, Kylander-Clark ARC, Hacker BR, Craddock JP (2017) The onset of the dead sea transform based on calcite age-strain analyses. *Geology* 45(7):587–590
- Omar GI, Steckler MS (1995) Fission track evidence on the initial rifting of the Red Sea: two pulses, no propagation. *Science* 270(5240):1341–1344
- Özbakir AD, Govers R, Wortel R (2017) Active faults in the Anatolian-Aegean plate boundary region with Nubia. *Turkish J Earth Sci*. <https://doi.org/10.3906/yer-1603-4>
- Pirouz M, Avouac J-P, Hassanzadeh J, Kirschvink JL, Bahroudi A (2017) Early Neogene foreland of the Zagros, implications for the initial closure of the Neo-Tethys and kinematics of crustal shortening. *Earth Planet Sci Lett* 477:168–182
- Reilinger R, McClusky S (2011) Nubia–Arabia–Eurasia plate motions and the dynamics of Mediterranean and Middle East tectonics. *Geophys J Int* 186(3):971–979
- Roobol MJ, Stewart ICF (2009) Cenozoic faults and recent seismicity in northwest Saudi Arabia and the Gulf of Aqaba region saudi geological survey technical report SGS-TR-2008 7 35
- Segev A, Lyakhovsky V, Weinberger R (2014) Continental transform–rift interaction adjacent to a continental margin: the Levant case study. *Earth Sci Rev* 139:83–103

- Segev A, Yoav A, Jacob S, Reli W (2017) Late Oligocene and Miocene different seaways to the Red Sea–Gulf of Suez rift and the Gulf of Aqaba–Dead Sea basins. *Earth Sci Rev* 171:196–219
- Steckler MS, ten Brink S (1986) Lithospheric strength variations as a control on new plate boundaries: examples from the northern Red Sea region. *Earth Planet Sci Lett* 79(1):120–132
- Stern RJ, Johnson PR (2019) Constraining the opening of the Red Sea Evidence from the Neoproterozoic margins and Cenozoic magmatism for a volcanic rifted margin. In: Najeeb MA, Rasul, Ian CF, Stewart (eds) *Geological setting Palaeoenvironment and archaeology of the Red Sea*. Springer, Cham, pp 53–79
- Stockli DF, William B (2019) Timing of extensional faulting along the magma-poor central and northern red sea rift margin—transition from regional extension to necking along a hyperextended rifted margin. In: Najeeb MA, Rasul, Ian CF, Stewart (eds) *Geological Setting Palaeobenvironment and Archaeology of the Red Sea*. Springer, Cham, pp 81–111
- Swanson MT (1982) Preliminary model for an early transform history in central Atlantic rifting. *Geology* 10(6):317–320
- Szymanski E, Stockli DF, Johnson PR, Hager C (2016) Thermochronometric evidence for diffuse extension and two-phase rifting within the Central Arabian margin of the Red Sea Rift. *Tectonics* 35(12):2863–2895
- Tubbs RE, Fouda HGA, Afifi AM, Raterman NS, Hughes GW, Fadolkareem YK (2014) Midyan Peninsula, northern Red Sea, Saudi Arabia: seismic imaging and regional interpretation. *GeoArabia* 19(3):165–184
- Ukstins IA, Renne PR, Wolfenden E, Baker J, Ayalew D, Menzies M (2002) Matching conjugate volcanic rifted margins: 40Ar/39Ar chrono-stratigraphy of pre-and syn-rift bimodal flood volcanism in Ethiopia and Yemen. *Earth Planet Sci Lett* 198(3–4):289–306
- Wessel P, Smith WHF (1991) Free software helps map and display data. *Eos, Transactions American Geophysical Union* 72(41):441–446
- Wilson M, Guiraud R (1992) magmatism and rifting in Western and Central Africa, from late jurassic to recent times. *Tectonophysics* 213(1–2):203–225
- Wolfenden E, Ebinger C, Yirgu G, Renne PR, Kelley SP (2005) Evolution of a volcanic rifted margin: southern red sea, ethiopia. *Geol Soc Am Bull* 117(7–8):846–864
- Wright TJ, Sigmundsson F, Pagli C, Belachew M, Hamling IJ, Brandsdóttir B, Keir D et al (2012) Geophysical constraints on the dynamics of spreading centres from rifting episodes on land. *Nat Geosci* 5(4):242–250

## Publisher's Note

Springer Nature remains neutral with regard to jurisdictional claims in published maps and institutional affiliations.

**Submit your manuscript to a SpringerOpen<sup>®</sup> journal and benefit from:**

- Convenient online submission
- Rigorous peer review
- Open access: articles freely available online
- High visibility within the field
- Retaining the copyright to your article

---

Submit your next manuscript at ► [springeropen.com](https://www.springeropen.com)